Presented at ICCE'94, Kobe, Japan, October 1994

CHAPTER 70

The application of load-cell technique in the study of armour unit responses to impact loads

Hans F. Burcharth[1] Zhou Liu[2]

Abstract

The slender, complex types of armour units, such as Tetrapods and Dolosse are widely used for rubble mound breakwaters. Many of the recent failures of such structures were caused by unforeseen early breakage of the units, thus revealing an inbalance between the strength (structural integrity) of the units and the hydraulic stability (resistance to displacements) of the armour layers. Breakage is caused by stresses from static, pulsating and impact loads. Impact load generated stresses are difficult to investigate due to non-linear scaling laws. The paper describes a method by which impact loads on slender armour units can be studied by load-cell technique. Moreover, the paper presents Dolos design diagrams for the prediction of both breakage and hydraulic stability.

Introduction

The slender complex types of armour units, such as Tetrapods and Dolosse are widely used. Breakage of the armour units has caused many of the recent breakwater failures. Thus there is a need for studying stresses in the units.

Due to the stochastic nature of the wave loads, the complex shape of the armour units and their random placement, the problem cannot be dealt with on a deterministic basis, but must be handled as a probabilistic problem.

Consequently, a very large number of situations must be investigated. This can be performed at reasonable costs only by small scale experiments. Stresses in small scale armour units are studied by the use of load-cells inserted in the units. Burcharth et al.(1992) presented design diagrams for structural integrity based on stress exceedence probability, which, however, do not express the proportion of the units that will break. The present paper presents a new set of diagrams for the prediction of the amount of breakage.

[1]Prof. of Marine Civil Engineering, Aalborg University, Denmark.
[2]Research Engineer, Ph.D. Aalborg University, Denmark.

Load-cell technique involves a number of complications. The installation of the load-cell makes the material properties of the unit different from those of the homogeneous prototype units and consequently the impact responses, which depend on the elastic behaviours of the bodies, cannot be directly reproduced in model tests. Besides this, the responses of the instrumented units could involve dynamic amplification effects. Moreover, the ultra short duration of solid body impact loads and the wave slamming necessitates high frequency sampling which results in data storage capacity problem. The frequencies of the impact stresses are in the order of 800-1500 Hz for the applied model units.

The paper first discusses the scale law for the impact stress in the armour units and presents results of impact calibration of the load-cell instrumented Tetrapods and Dolosse. The paper then presents the model test results on impact stresses of Dolosse and finally presents the design diagrams which incorporate both the hydraulic stability and the structural integrity of Dolos armour layers. The diagrammes are different from the earlier ones presented by the authors in that they contain information on the proportion of the units that will break, instead of the stress exceedence probability.

Duration of impacts

When two solid bodies collide the impact force and the related stresses will depend on the duration of the impact, i.e. the time of contact, τ. Due to the non-linear material properties of concrete and to the complex shape of slender armour units it is not possible to establish a formula by which τ can be quantified. However, it is sufficient for the present research to formulate a qualitative expression for τ. In the following are discussed two realistic models for estimation of τ. It is shown that for geometrically similar systems and constant Poisson's ratio it is reasonable to assume

$$\tau \sim L\sqrt{\frac{\rho_A}{E_A}} \tag{1}$$

where $\sim$ means proportional to.

Case 1. Impacting blunt bodies of identical linear elastic material.

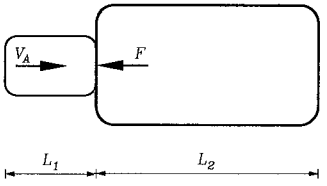

L_1 and L_2 are proportional to the characteristic length L of the system.

It is assumed that the impact generates mainly one-dimensional compression

longitudinal shock waves which travel with the rod wave speed, $C = \sqrt{E_A/\rho_A}$, the distances L_1 and L_2 to the free edges, where they are reflected as tension waves. The two bodies will loose contact at the first return of a tension wave to the impact surface. Consequently, because $L_1 < L_2$

$$\tau = \frac{2\,L_1}{C} = \frac{2\,L_1}{\sqrt{\frac{E_A}{\rho_A}}} \qquad \text{or} \qquad \tau \sim L\sqrt{\frac{\rho_A}{E_A}}$$

Case 2. Slender body impacted by blunt body of identical linear elastic material.

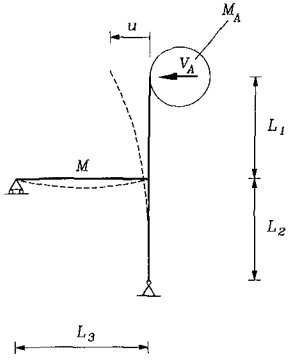

$$L_1 \sim L_2 \sim L_3 \sim L$$
$$M \sim M_A \sim \rho_A L^3$$

The impacting blunt body of mass M_A hits the slender structure of mass $M \sim M_A$ with impact velocity V_A by which a vibration mainly caused by bending and shear is initiated. It is assumed that the maximum value of τ corresponds to contact between the two bodies during approximately one half period T of the first mode of vibration for the slender body.

If it is assumed that the slender structure has a linear response corresponding to transverse impacts on free and simply supported beams then the system corresponds in principle to a mass-spring system with spring stiffness

$$k \sim \frac{E_A I}{L^3} \tag{2}$$

where $I \sim L^4$ is the moment of inertia.

The deflection time defined as one half period of the first mode of vibration is

$$\tau \simeq \frac{T}{2} \simeq \sqrt{\frac{M_A + M_o}{k}} \tag{3}$$

where $M_o \sim M \sim M_A \sim \rho_A L^3$ is the modal mass of the slender body.

From eqs (2) and (3) is then obtained eq (1). This conclusion was already presented in Burcharth (1984).

Scaling law for impact stresses of armour units

Case 1. Scale law in case of free fall impinging body

Geometrical similarity and constant coefficient of restitution are assumed

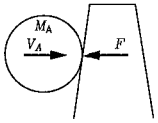

$$V_A \sim \sqrt{2g\,L}$$
$$M_A \sim \rho_A\,L^3 \tag{4}$$

The momentum equation reads

$$F\,\tau = M_A\,\Delta\,V_A \sim M_A\,V_A \tag{5}$$

where τ is the duration of the impact and ΔV is the velocity difference of the impinging body before and after the collision. $\Delta V \sim V_A$ is due to the assumed constant coefficient of restitution.

Inserting eqs (1) and (4) in eq (5) yields

$$F \sim \frac{\rho_A\,L^3\,(g\,L)^{0.5}\,E_A^{0.5}}{L\,\rho_A^{0.5}} = \rho_A^{0.5}\,E_A^{0.5}\,g^{0.5}\,L^{2.5}$$

Introducing $\lambda = \dfrac{\text{model value}}{\text{prototype value}}$ we obtain

$$\lambda_{\sigma_{Impact}} = (\lambda_{\rho_A}\,\lambda_{E_A}\,\lambda_L\,\lambda_g)^{0.5} \tag{6}$$

Case 2. Scale law of impinging body affected only by flow forces

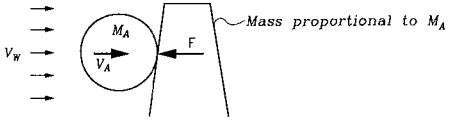

V_A is found from Newton's equation

$$F_W = M_A \frac{d\,V_A}{dt} \tag{7}$$

$$V_A = \frac{F_W}{M_A}\,t = \frac{F_W}{\rho_A\,L^3}\,t \tag{8}$$

where F_w is the flow force on the impinging body.

By the use of eqs (1), (5) and (8) is obtained

$$F \sim \frac{\rho_A L^3 F_W t E_A^{0.5}}{\rho_A L^3 L \rho_A^{0.5}} = \rho_A^{-0.5} L^{-1} F_W t E_A^{0.5}$$

$$\lambda_{\sigma_{Impact}} = \lambda_{\rho_A}^{-0.5} \lambda_L^{-3} \lambda_{F_W} \lambda_t \lambda_{E_A}^{0.5} \tag{9}$$

Because in the Froude model, $\lambda_{F_W} = \lambda_{\rho_W} \lambda_L^3$ and $\lambda_t = \lambda_L^{0.5}$, then

$$\lambda_{\sigma_{Impact}} = \lambda_{\rho_A}^{-0.5} \lambda_{\rho_W} \lambda_{E_A}^{0.5} \lambda_L^{0.5} \tag{10}$$

The variation in F_w due to viscous effects is neglected. This, however, introduces some unknown bias, the size of which depends on the Reynolds number range.

Case 3. Collision between impinging water (slamming) and a solid body.

The air-cushioning effect is neglected because it is unlikely that air-pockets will be entrapped due to the limited size and rounded shape of the elements.

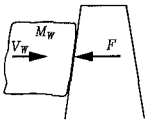

$$\begin{aligned} V_W &\sim \sqrt{g L} \\ M_W &\sim \rho_W L^3 \end{aligned} \tag{11}$$

τ is assumed given by (1) because the solid body stress wave is reflected from a free surface of the armour unit long time before reflection from a free surface of the wave (travel distance $\simeq H_s >$ dimension of armour unit; shock wave speed is smaller in water than in concrete) and the deflection time will be shorter than the transverse time of the elastic wave in the water.
From the momentum equation

$$F \tau = M_W \Delta V_W \sim M_W V_W \tag{12}$$

and eqs (1) and (8) is obtained

$$F \sim \frac{\rho_W L^3 g^{0.5} L^{0.5} E_A^{0.5}}{L \rho_A^{0.5}} = \rho_A^{-0.5} \rho_W E_A^{0.5} L^{2.5} g^{0.5}$$

and consequently

$$\lambda_{\sigma_{Impact}} = \lambda_{\rho_A}^{-0.5} \lambda_{\rho_W} \lambda_{E_A}^{0.5} \lambda_L^{0.5} \lambda_g^{0.5} \tag{13}$$

The difference between the above three scaling laws eqs (6), (10) and (13) is related to the scales of the densities only, because generally

$$\lambda_{\rho_A} \neq \lambda_{\rho_A}^{-0.5} \lambda_{\rho_W} \tag{14}$$

As long as the model is made of approximately the same concrete as the prototype, eq (6) can be chosen as the scaling law for the impact stresses, as it introduces less than 1% error for $0.97 \leq \lambda_{\rho_A} \geq 1.00$ and $0.98 \leq \lambda_{\rho_w} \geq 1.00$.

Apparent elasticity of the units with load-cell

The scaling law for the impact stresses of armour units is related to the elasticity of the material. Unfortunately, the insertion of the load-cell destroys the homogeneity of the material. This means that the impact stresses recorded in the small scale model tests cannot be scaled up to prototypes by the use of eq (6) valid only for homogeneous materials. Fig.1 shows the 200 g Dolos and 280 g Tetrapod with the load-cells.

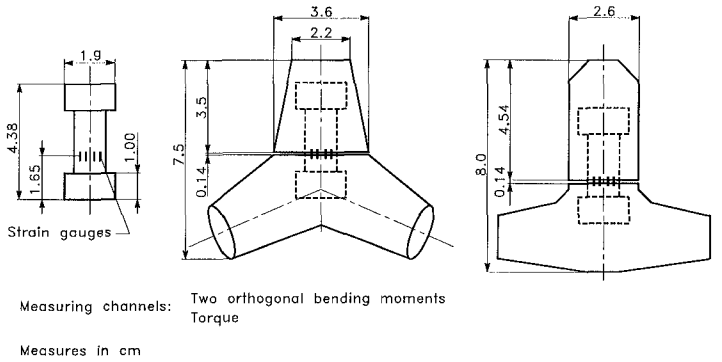

Fig.1. 200 g Dolos and 280 g Tetrapod with the load-cells.

However, by comparison of small scale impact test results for Dolosse and Tetrapods with results of the similar large scale impact tests (Burcharth, 1980, Bürger et al. 1990), it is possible to obtain an apparent elasticity for the small scale units. The apparent elasticity is then used for the interpretation of the impact signals recorded in the hydraulic flume tests.

The impact calibration results of the small scale Dolosse with load-cell have been published in Burcharth et al.(1990). The results of impact calibration of the Tetrapods are given in Fig.2. For the applied pendulum test set-up the reference is made to Bürger et al.(1990).

A way of checking the apparent elasticity is to compare the impact duration of the small load-cell mounted units with those of the various large size units, cf. eq (1). Fig.3 shows the ratio of dimensionless stress of various sizes of Dolosse using the apparent elasticity of the 200 g Dolos. Even though there is a big scatter, it can be seen that most ratios are around the value of 1, thus confirming the value of the apparent elasticity.

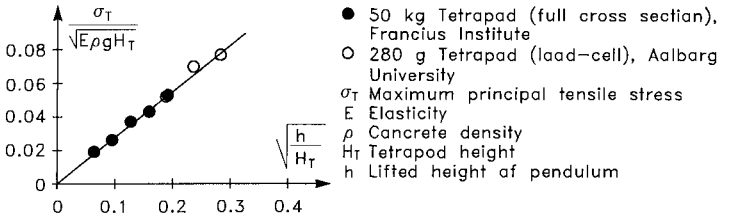

Fig. 2. Comparison of pendulum test results of the large scale Tetrapod with surface mounted strain gauges and the small scale Tetrapod with load-cell. Apparent elasticity $E = 4799\ MPa$.

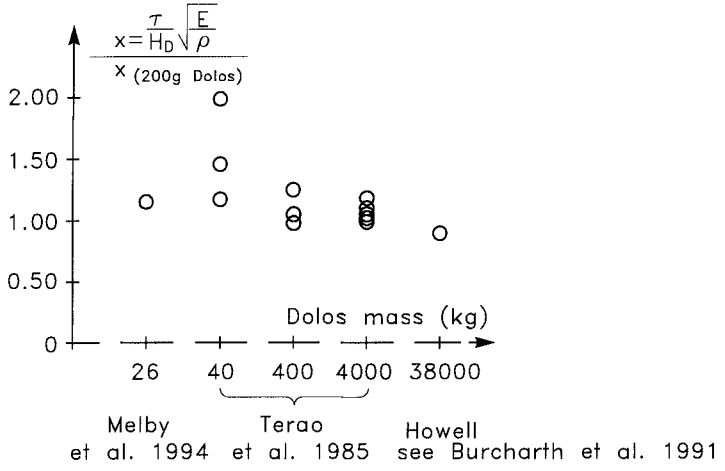

Fig. 3. Ratios of the dimensionless impact duration of large scale Dolosse against 200 g Dolos with load-cell. Apparent elasticity $E = 3500\ MPa$.

Sampling frequency

The ultra short duration of solid body impact loads and wave slamming requires a very high sampling frequency. The following analysis gives the underestimation of the stress corresponding to a certain sampling frequency.

Suppose the stress signal is recorded at frequency f_s and the stress signal is sinusoidal with the maximum stress σ_p and the frequency f.

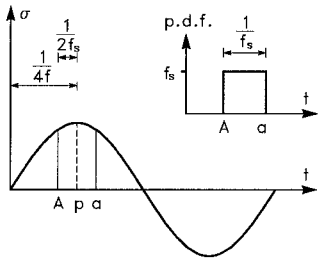

$$\sigma = \sigma_p \sin(2\pi f t) \tag{15}$$

Fig. 4. Sinusoidal stress signal.

The most unfavourable case is when the two adjacent sampling points, A and a, are symmetrically located around the center of the peak p. For this case the sampled maximum stress σ_A is

$$\sigma_A = \sigma_p \sin(2\pi f t_A) = \sigma_p \sin\left(2\pi f\left(\frac{1}{4f} - \frac{1}{2f_s}\right)\right) \tag{16}$$

and *the maximum relative error* is

$$\frac{\sigma_p - \sigma_A}{\sigma_p} = 1 - \sin\left(\pi\left(\frac{1}{2} - \frac{f}{f_s}\right)\right) \tag{17}$$

On the other hand, if the sampling points are uniformally distributed along the length (A-a), the average of the sampled maximum stress is

$$\begin{aligned}\overline{\sigma} &= \int_{t_A}^{t_a} \sigma_p \sin(2\pi f t) f_s \, dt \\ &= \frac{\sigma_p}{2\pi} \frac{f_s}{f}\left(\cos\pi\left(\frac{1}{2} - \frac{f}{f_s}\right) - \cos\pi\left(\frac{1}{2} + \frac{f}{f_s}\right)\right)\end{aligned} \tag{18}$$

and *the average relative error* is

$$\frac{\sigma_p - \overline{\sigma}}{\sigma_p} = 1 - \frac{1}{2\pi} \frac{f_s}{f}\left(\cos\pi\left(\frac{1}{2} - \frac{f}{f_s}\right) - \cos\pi\left(\frac{1}{2} + \frac{f}{f_s}\right)\right) \tag{19}$$

The maximum relative error and the average relative error are depicted in Fig.5. However, the actual impact signals are not sinusoidal, cf. Fig.6. In order to check the influence of the sampling frequency a series of Dolos pendulum tests with different sampling frequencies have been performed. The results are depicted in Fig.6. It can be seen that the sinusoidal results hold also for the actual impact signal when the offset for $f_s = 10000\ Hz$ is considered.

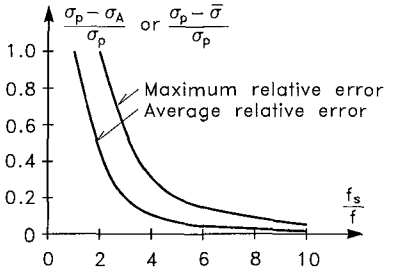

Fig. 5. Maximum relative error and average relative error due to the limited sample frequency.

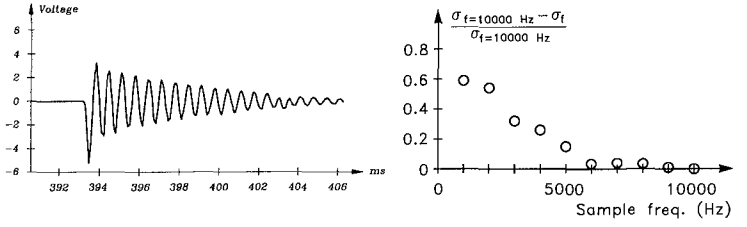

Fig. 6. Example of the impact signals of the 200 g load-cell instrumented concrete Dolosse ($f = 1500\ Hz$) and the relative error of the Dolos pendulum test results as function of the sampling frequency.

In the Dolos hydraulic model test, the applied sampling frequency is $f_s = 6000\ Hz$ and the damped natural frequency of the instrumented Dolosse $f = 1500\ Hz$. On average the sampled maximum impact stress is underestimated by 10% due to the limited sampling frequency. Therefore, in the data processing all sampled maximum impact stresses were increased by 10% .

Check for the dynamic amplification by wave slamming

It is well-known that resonance occurs when the frequency of the load is close to the natural frequency of the system. The installation of the load-cell into the model Dolos makes its natural frequency smaller, cf. eq (1). In order to check if the reduced natural frequency of the Dolosse is close to the wave slamming frequency, and hence introduces dynamic amplification, the frequency of the wave slamming on the Dolos armour layer was recorded by a pressure transducer installed in the stem of the Dolos. The pressure transducer did in all tests face the breaking waves. The results are given in Fig.7, showing the highest frequency of the wave slamming on the Dolos armour to be 330 Hz, far away from the

natural frequency of 1500 Hz for the Dolosse with the load-cells. Consequently, no dynamic amplification are present in the model tests.

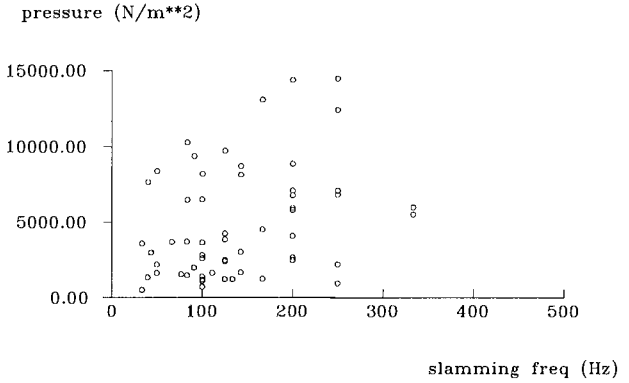

Fig. 7. Recorded frequencies of the wave slamming on the Dolos armour units.

Description of the experiments

A 1 : 1.5 slope armoured with 200 g concrete Dolosse of waist ratios 0.325, 0.37 and 0.42 were exposed to irregular waves in a wave flume with a foreshore slope of 1 : 20. Fig. 8 shows the set-up of the model and the cross section of the breakwater. The hydraulic stability formula of Dolos armour layer is given by (Burcharth et al. 1992)

$$N_s = \frac{H_s}{\Delta D_n} = (47 - 72\,r)\,\varphi_{n=2} D^{1/3} N_z^{-0.1}$$

$$= (17 - 26\,r)\,\varphi_{n=2}^{2/3} N_{od}^{1/3} N_z^{-0.1} \qquad (20)$$

where H_s significant wave height in front of breakwater

Δ $(\rho_{concrete}/\rho_{water}) - 1$, ρ is the mass density

D_n length of cube with the same volume as Dolosse

r Dolos waist ratio

$\varphi_{n=2}$ packing density

D relative number of units within levels SWL $\pm$ 6.5 Dn displaced one Dolos height h, or more (e.g. for 2% displacement insert $D = 0.02$)

N_{od} number of displaced units within a width of one equivalent cubic length D_n.

N_z number of waves. For $N_z \geq 3000$ use $N_z = 3000$.

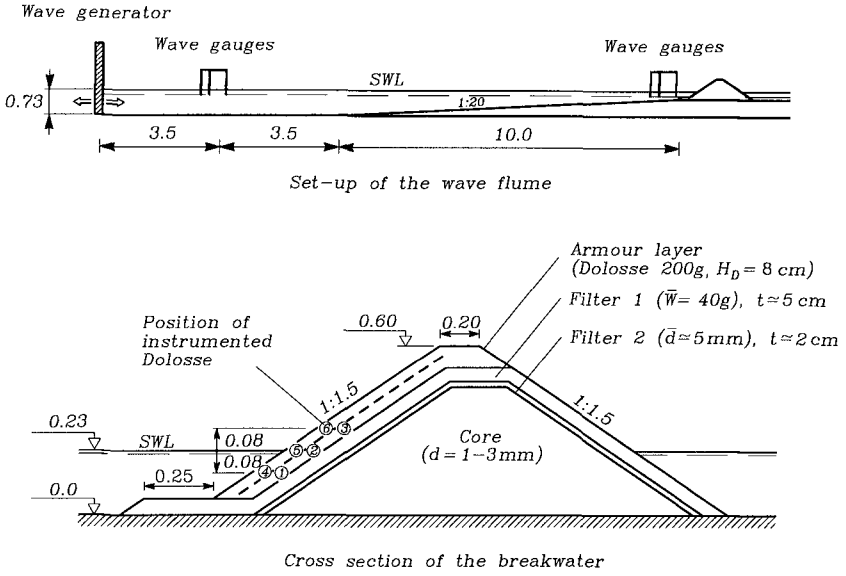

Fig. 8. Set-up of the wave flume and the cross section of the breakwater.

Distribution of stresses over the slope

The distribution of σ_T over the slope is of interest in order to identify the potential areas for armour breakage.

Fig. 9 shows typical distributions given by the 2% exceedence values of σ_T for each of the six instrumented Dolos positions for 10 t and 50 t Dolos of waist ratios 0.325 and 0.42 exposed to wave action levels, $N_S = \dfrac{H^t_{m_o}}{\Delta D_n} = 0.9$, 1.8 and 2.6.

The following conclusions can be drawn from the analyses of a large number of distributions of maximum σ_T over the slope:

- The contribution of the impact stress to the maximum principal tensile stress σ_T is small for $N_S \leq 2.0$.
- The contribution from the impact stress to σ_T is small in the bottom layer.
- The contribution from the impact stress to σ_T is very significant in the top layer.
- Breakage will in most cases start in the top layer in the zone just below SWL. This zone is more vulnerable to breakage than the zone above SWL.

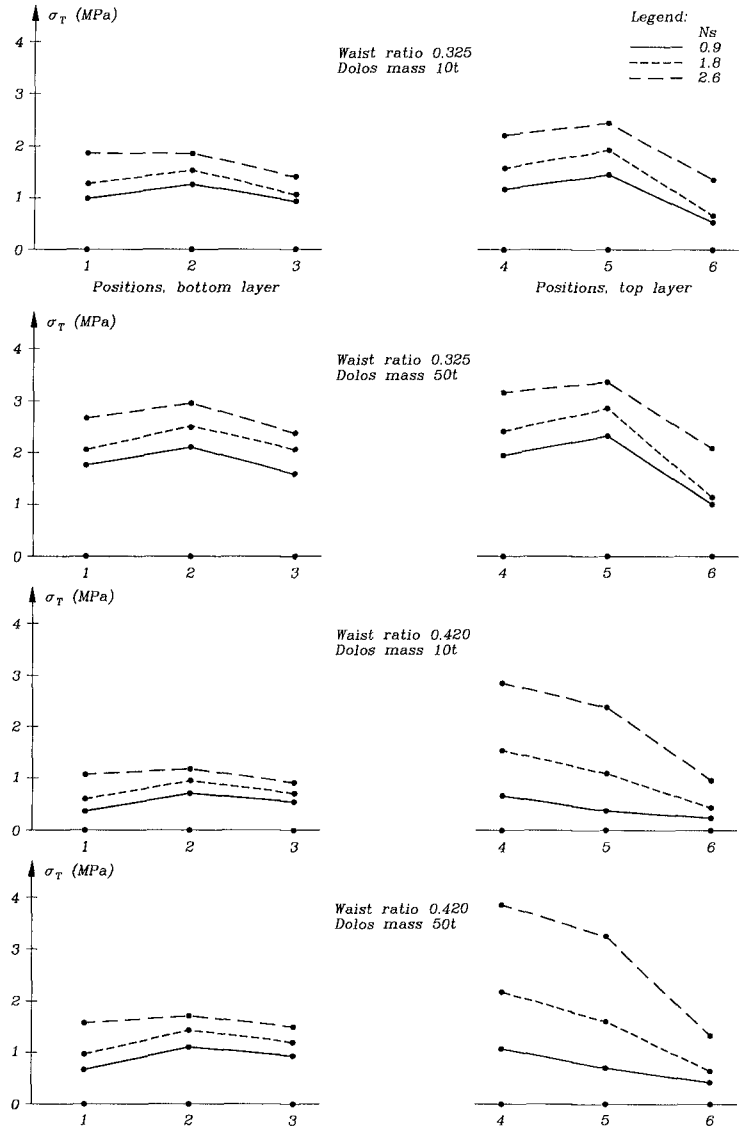

Fig. 9. Distribution of σ_T over the slope, Dolos positions 1 to 6, cf. Fig. 8. 2% stress exceedence probability level.

Design diagramme

In the analysis of breakage it is only the maximum value of σ_T in each instrumented Dolos within a test run which is of interest. Repeated short test runs of 100-300 waves were used because most movements take place in the beginning of each test.

The authors presented Dolos design diagrammes in ICCE'92 based on stress exceedence probability, which do not give exactly the proportion of the units that will break. A reanalysis was performed in which the maximum stress of each load-cell instrumented Dolos within each test run was compared with the strength of concrete in order to obtain the relative number of units that will break.

The results are given in the design diagrams, one of which is shown in Fig.10. For the complete set of the design diagrams reference is made to Burcharth (1993).

The concrete tensile strength in the diagrams is the one corresponding to static load. However, the diagrams take into account the dynamic amplification of the strength when impacts are involved.

The design diagrams have been checked against observed behaviour of prototype Dolos breakwaters and good agreement was found, cf. Table 1.

Table 1. Observed and predicted damage of some Dolos breakwaters

	Crescent City USA	Richards Bay SA	Sines POR
H_s (m)	10.7 (1)	5 (2)	9 (3)
slope	1:4	1:2	1:1.5
Dolos mass (ton)	38	20	42
Waist ratio	0.32	0.33	0.35
Dolos packing density	0.85	1	0.83
Concrete density (kg/m^3)	2500	2350	2400
Elasticity (MPa) (4)	30,000	30,000	30,000
Tensile strength (MPa) (4)	3	3	3
Reported displacement	7.3%		
Reported breakage	19.7%		
Reported displacement+breakage	26.8%	4%	collapse
Predicted displacement	3.6%	0.6%	3.6 %
Predicted breakage	> 10%	5%	> 10%

(1) depth limited in front of breakwater
(2) in front of breakwater
(3) offshore ≈ in front of breakwater
(4) estimated values

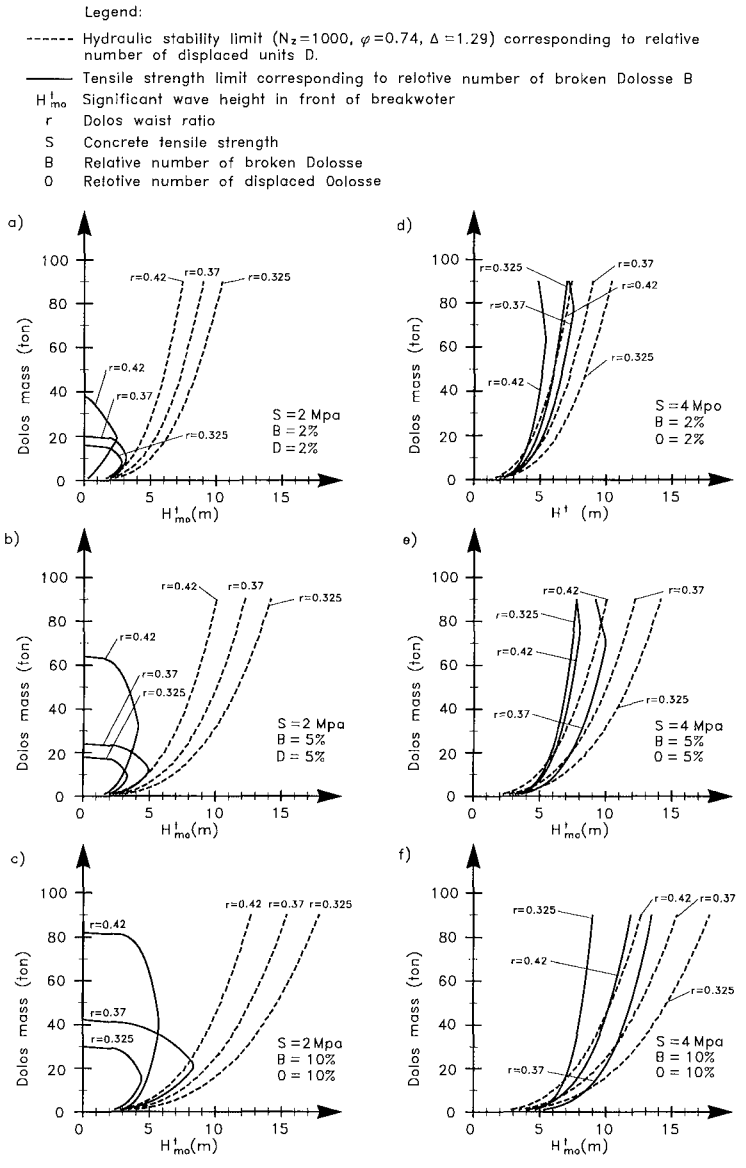

Fig. 10. Design diagrams for structural integrity and hydraulic stability of Dolos armour. Reference area SWL $\pm 6.5D_n$.

Acknowledgements

The load-cells applied in this study were kindly made available by CERC, USA. The project was partly sponsored by the Commission of the European Community under the Marine Science And Technology Research Program (MAST II), and partly sponsored by the Danish Technical Research Council under the MARIN TEKNIK Research Program.

References

Burcharth, H.F. (1981). Full-scale dynamic testing of Dolosse to destruction. Coastal Engineering, 4 (1981).

Burcharth, H.F. (1984). Fatigue in breakwater armour units. Proceedings of the 19th International Conference on Coastal Engineering, Houston, Texas, 1984.

Burcharth, H.F. and Liu, Z.(1990). A general discussion of problems related to the determination of concrete armour unit stresses inclusive specific results related to static and dynamic stresses in Dolosse. Proc. Seminar on Structural Response of Armour Units. CERC, Vicksburg, MISS, USA.

Burcharth, H.F., Howell, G.L. and Liu, Z.(1991). On the determination of concrete armour unit stresses including specific results related to Dolosse. Coastal Engineering, 15 (1991), pp 107-165.

Burcharth, H.F. and Liu, Z. (1992). Design of Dolos armour units. Proceedings of the 23rd International Conference on Coastal Engineering. Venice. Italy.

Burcharth, H.F. (1993). Structural integrity and hydraulic stability of Dolos armour layers. Series Paper 9, published by the Department of Civil Engineering, Aalborg University, Denmark, 1993

Bürger, W.W., Oumeraci, H., Partenscky, H.W. (1990). Impact strain investigations on tetrapods results of dry and hydraulic tests. ASCE Proc. Seminar Stresses in Concrete Armor Units.

Melby, J.A. and Turk, G.F. (1994). Scale and modeling effects in concrete armor experiments. Coastal Dynamics'94, Barcelona, Spain.

Terao, T., Terauchi, K., Ushida, S., Shiraishi, N., Kobayashi, K. and Gahara, H. (1985). Prototype testing of Dolosse to destruction. Proc. Workshop on Measurement and Analysis of Structural Response in Concrete Armor Units. U.S. Army Corps of Engineers, CERC, WES, Vicksburg, MISS., USA.